Hindawi
Science and Technology of Nuclear Installations
Volume 2019, Article ID 4930274, 13 pages
https://doi.org/10.1155/2019/4930274

Research Article

Transmutations of Long-Lived and Medium-Lived Fission Products Extracted from CANDU and PWR Spent Fuels in an Accelerator-Driven System

Alper Buğra Arslan,[1] **İlayda Yilmaz**,[1] **Gizem Bakir**,[2] **and Hüseyin Yapici**[1]

[1]*Erciyes Üniversitesi Mühendislik Fakültesi, 38039 Kayseri, Turkey*
[2]*Cumhuriyet Üniversitesi Teknoloji Fakültesi, 58140 Sivas, Turkey*

Correspondence should be addressed to Alper Buğra Arslan; alperbugraarslan@gmail.com

Received 12 July 2019; Revised 29 August 2019; Accepted 17 September 2019; Published 20 October 2019

Academic Editor: Arkady Serikov

Copyright © 2019 Alper Buğra Arslan et al. This is an open access article distributed under the Creative Commons Attribution License, which permits unrestricted use, distribution, and reproduction in any medium, provided the original work is properly cited.

This study presents the time-dependent analyses of transmutations of long-lived fission products (LLFPs) and medium-lived fission products (MLFPs) occurring in thermal reactors in a conceptual helium gas-cooled accelerator-driven system (ADS). In accordance with this purpose, the CANDU-37 and PWR 15 × 15 spent fuels are separately considered. The ADS consists of LBE-spallation neutron target, subcritical fuel zone, and graphite reflector zone. While the considered ADS is fueled with the spent nuclear fuels extracted from each thermal reactor without the use of additional fuel, fission products extracted from same thermal reactor are also placed into transmutation zone in graphite reflector zone. The LLFP transmutation performance of the modified ADS is analyzed by considering three different spent fuels extracted from the thermal reactors. Spent fuels are extracted from CANDU-37 in case A, from PWR-15 × 15 in case B, and from CANDU-37 fueled with mixture of PWR 15 × 15 spent fuel and 46% ThO_2 in case C. The LBE target is bombard with protons of 1000 MeV. The proton beam power is assumed as 20 MW, which corresponds to $1.24828 \cdot 10^{17}$ protons per second. MCNPX 2.7 and CINDER 90 computer codes are used for the time-dependent burn calculations. The ADS is operated under subcritical mode until the value of k_{eff} increases to 0.984, and the maximum operation times are obtained as 3400, 3270, and 5040 days according to the spent fuel cases of A, B, and C, respectively. The calculations bring out that in the modified ADS, LLFPs and MLFPs, which are extracted from thermal reactors, can be transformed to stable isotopes in significant amounts along with energy production.

1. Introduction

The CANDU reactors, firstly developed in Canada, are commercial thermal reactors that mainly use natural uranium as fuel. Their cooler and moderator are high-pressured liquid heavy water (D_2O). The CANDU reactors do not use control rods that regulate the neutron numbers in the reactor. Furthermore, these reactors can be refueled during full-power operation. Another commercial thermal reactor type is PWR that is fueled with the enriched uranium (3%–4%). These reactors are cooled and moderated by high-pressure liquid light water (H_2O). PWR and CANDU reactors are the most used reactor types in electricity generation. However, the spent fuels of these reactors contain abundant amounts of fertile fuel, which cannot be used for energy generation, and large amounts of hazardous radioactive nuclear waste. Most of the spent fuels of the nuclear power plants are fertile and fissile and they are still valuable, and can become reusable by rejuvenating in accelerator-driven systems (ADSs). Nuclear wastes also include highly radioactive long-lived fission products (LLFPs). Therefore, the spent fuel management is one of the most crucial problems of nuclear energy industry. In order to solve these spent fuel problems, a new and innovative approach, instead of deep geological storages of nuclear waste and LLFPs, is presented where nuclear waste is transmuted into stable isotopes in ADSs.

Some fission products may have a short half-life, while others have half-lives of 100 years, 1000 years, or millions of years. If half-life of a radioactive isotope is beyond 30 years, these isotopes are called long-lived isotopes in terms of nuclear waste management. LLFPs can be transmuted into stable isotopes via neutron/proton interaction reactions in suitable nuclear reactors. Yapıcı and Özışık [1] have analyzed the LLFP transmutation and fissile breeding in the Prometheus reactor. ^{99}Tc, ^{129}I, and^{135}Cs isotopes are placed separately in the transmutation zone, and ceramic uranium mono carbons (U-C) are used as fuels in the fissile breeding zone. They used the XSDRNPM/SCALE4.4a neutron transport code and the MCNP4B Monte Carlo code for neutronic calculations. They achieve effective fissile breeding, LLFP transmutation, and energy production. Yapıcı et al. [2] have studied on transmutation of LLFP and minor actinide (MA) discharged from high burnup PWR-MOX spent fuel in fusion-driven transmuter. They have investigated the effect of volume rate of MA and LLFPs on transmutation. They have designed two different transmutation zones for MA and LLFP. The results show that the transmutation rate of LLFPs increased by the increase of the volume rates of the MA's, and ^{99}Tc has the highest transmutation rate. Yapıcı et al. [3] investigated time-dependent transmutation of LLFP and MA high-level waste in fusion-driven transmuters. They consider PWR mixed-oxide MOX spent fuel as high-level waste and design separate transmutation zones for MAs and LLFPs. As a result, they have significantly reduced the effective half-lives of the MA and LLFP nuclide. Igashira and Ohsaki [4] have worked to transmute various LLFPs into stable and short-lived isotopes in FBR (fast breeder reactor). They investigate reactions (n, γ) and $(n, 2n)$ of LLFP using JENDL-3.2 and ENDF/B-VI codes. 0.25 neutrons per fission are required for isotopic separation of the LLFPs, while 6.8 neutrons are necessary for chemical separation. Liu et al. [5] have conducted a systematic study on the transmutation of LLFPs in PWR and have aimed to develop an optimal transmutation strategy for nuclear energy development. They examine transmutation of LLFP discharged from LWR. In the results, they see that ^{99}Tc and ^{129}I could be transformed in the present PWRs in the form of target pins. Setiawan and Kitamoto [6] have studied on the effective transmutation of LLFPs in LWR to BWR and PWR and they compare BWR and PWR. Iodine and technetium transmutation in the BWR is found to be more effective than in the PWR. The time required for transmutation of 30–40 percent of ^{99}Tc and ^{129}I is estimated to be 10–15 years and 30–40 years, respectively. Wakabayashi [7] worked on the transmutation of MA and LLFP in the fast reactor and achieved maximum fission product transmutation by using Duplex pellets in the target. The results show that LLFP and MA perfectly transmute in the fast reactor. Kora et al. [8] consider 4 different HTGR to convert LLFPs. Their aim is LLFP transmutation and storage, and they realize effective LLFP transmutation. Takiyabev et al. [9] investigate the LLFP transmutation at the fusion neutron source. The thermal flux of the fusion neutron source has been proven for the transmutation of the most difficult LLFPs of the blanket potential. They have effectively transformed ^{93}Zr.

The ADSs operated under subcritical mode are reactors that have high power production potential. In an ADS, the target is bombarded with high energetic protons, which in turn produces tens of neutrons. Sarer et al. [10] design a high-energy proton accelerator for ^{99}Tc, ^{129}I long-life fuel products, ^{237}Np and ^{241}Am minor actinides, and the conversion of ^{239}Pu. They choose natural lead as target material and use 1 GeV of proton. They use the MCNPX code in neutronic calculations. In the conclusion, they have seen that both used fuels are converted, and energy is obtained. As a result, they realized both the transmutation of spent fuel and energy production. Kawase et al. [11] have worked on the spallation reactions of ^{93}Zr, the long-life fission product, to provide simple data requirements for nuclear waste transmutation. In RIKEN Radioactive Isotope Beam Factory, inverse kinematics has been measured at 105 MeV/nucleon. Comparing the experimental studies with the PHITS calculations, they found that there were more products estimated in the intranuclear cascade and evaporation processes. As a result of the study, it has been found that spallation reactions can be a solution to stabilizing ^{93}Zr. Han et al. [12] investigate the transmutation of ^{126}Sn in the target of ADS. They use the cylindrical liquid ^{126}Sn target and investigate spallation product accumulation and neutron production. They have calculated that 40 neutrons are produced per 1.5 GeV proton. They have also seen that the effective half-life of ^{126}Sn is reduced. Yang et al. [13] conduct a systematic study to find the optimal solution for LLFP transmutation. They considered PWR core and sodium-cooled accelerator for ^{99}Tc and^{129}I transmutation. Various targets and loading optimization have been done to achieve the optimum transmutation, and^{99}Tc and ^{129}I were stabilized. Landeyro and Guidotti [14] investigate the transmutation of minor actinide and LLFP (only ^{99}Tc) in ADS to make radioactive waste safe. Two Monte Carlo calculation models have been developed to define critical safety conditions and the burning capacities of MA and Pu. The results show that LLFPs can be confidently transformed. Yapici et al. [15] investigate high-level waste transmutation (HWL) and potential of fissile production in various ADSs cooled with LBE. They select ^{99}Tc, ^{129}I, and^{135}Cs as high-level waste and use uranium carbide including high-level fissile fraction (10%–24%) as fuel. They use MCNPX code in neutronic calculations. The results show that they obtain effective LLFP conversion performance, fissile breeding, and energy production in optimized ADS.

The reviewed studies generally include the transmutations of MA and/or FPs. In this study, in a conceptual helium gas-cooled ADS with LBE target, the time-dependent transmutation analyses of FPs extracted from the CANDU-37 and PWR 15×15 spent fuels are investigated separately. These spent fuels are taken from reference [16]. The ADS design in our previous study [17] is modified for the transmutation of LLFPs and MLFPs. Furthermore, difference of this study from [13–15] is that there is no extra fissile fuel input to whole system (ADS and thermal reactor). Particularly, only thorium fuel enters into the system from outside of the system. Furthermore, in this study, more number of FPs (eleven FPs) are transmuted with respect to

the studies in [13–15] as number of FP. They analyzed maximal three FPs (^{99}Tc, ^{129}I, and ^{135}Cs) in their studies.

2. Helium Gas Coolant Accelerator-Driven System

In this work, to transmute LLFPs and MLFPs extracted from the spent fuel of thermal reactors into stable isotopes, the helium gas coolant accelerator-driven system used in previous study [17] is modified. The LBE target is bombard with protons of 1000 MeV. The proton beam power is assumed as 20 MW, which corresponds to $1.24828 \cdot 10^{17}$ protons per second. As is apparent from Figures 1(a) and 1(b), as distinct from original ADS, which includes only fuel zone [17], a transmutation zone including the LLFPs and MLFPs is embedded in the blanket of original ADS. This ensures that LLFPs and MLFPs can be effectively transmuted by means of neutrons from fuel zone.

The modified ADS consists of four parts as follows:

(i) LBE-spallation neutron target (SNT)

(ii) Subcritical fuel zone (SCFZ)

(iii) Transmutation zone (TZ)

(iv) Graphite reflector zone (GRZ)

2.1. Spallation Neutron Target. When the target of an ADS is bombarded with high energetic protons, it is desired that as many neutrons as possible are released. In this study, lead-bismuth eutectic (LBE, 44.5% lead and 55% bismuth), which is the most favored for ADS applications because of very good neutronic, chemical, and thermal properties, is used as the target material. The protons, whose energies are amplified in linear accelerator (LINAC), uniformly impact on the target material with a radius of 4 cm.

2.2. Subcritical Fuel Zone. The fresh fuels of CANDU-37 and PWR 15×15 are natural and enriched UO_2, which include 0.71% and 4.72% ^{235}U, respectively. The spent fuel rods extracted from these thermal reactors and containing uranium and transuranium isotopes are placed into this zone in a hexagonal arrangement. In this study, three different nuclear fuel compositions, which are taken from [16], are considered as follows:

(i) Case A: the fuel is the CANDU-37 spent fuel, which is burned 180 days and then cooled 720 days. Its total mass is 10.165 tHM.

(ii) Case B: the fuel is the PWR 15×15 spent fuel, which is burned 900 days and then cooled 720 days. Its total mass is 9.151 tHM.

(iii) Case C: the fuel is the CANDU-37 spent fuel, which is burned 180 days and then cooled 720 days. However, in this case, different from Case A, the CANDU-37 fuel is the mixture of 46% ThO_2 with 900 days burned and 720 days cooled 54% PWR 15×15 spent fuel. Its total mass is 8.748 tHM.

Volume fractions (VFs) of the fuel, fuel clad, and coolant (helium gas) are 60%, 8.5%, and 31.5%, respectively.

2.3. Transmutation Zone. In each fuel case mentioned above, some important LLFPs (half-life are more than 200,000 years) and MLFPs (half-life are shorter than 100 years) extracted from the spent fuel are placed into cylindrical rods made of zircaloy. The rods are placed into TZ in a hexagonal arrangement to transmute these fission products. VFs of fission products, rod clad, and graphite container are 60%, 8.5%, and 31.5%, respectively.

2.4. Graphite Reflector Zone. This zone, made of graphite, serves reflecting and returning of neutrons escaping SCTZ to increase transmutation reactions. In graphite-neutron interaction, the ratio of scatter cross section to absorption cross section is much higher than 1. Furthermore, graphite has a high-temperature-resistant property. Therefore, it is an attractive material for nuclear applications as neutron reflector and moderator material.

3. Time-Dependent Numerical Analyses

3.1. Calculation Method. Numerical analyses are performed by using the MCNPX 2.7 computer code [18] along with Los Alamos 150 MeV transport library (LA150) developed for computational simulations of ADSs by Chadwick et al [19]. Monte Carlo N-Particle Transport Code (MCNP), which can simulate nuclear processes in three dimensions, is written by Los Alamos National Laboratory. This library includes nuclear reaction cross sections and emission spectra up to 150 MeV for incident neutrons/protons for over 40 isotopes. Bertini INC model is used for the simulation of intranuclear cascade of spallation reactions. Furthermore, the CINDER 90 computer code [20] integrated with MCNPX 2.7 is used for the time-dependent burnup/depletion calculations. The outputs of MCNPX 2.7 and CINDER 90 computer codes are postprocessed with XBURN [21] and CBURN [22] interface computer codes, respectively.

3.2. General Neutronic Data

3.2.1. Effective Neutron Multiplication Factor. In nuclear reactors, effective neutron multiplication factor (k_{eff}) is defined as the ratio of number of neutrons in one generation to number of neutrons in preceding generation. The increase in k_{eff} during operation times are plotted in Figure 2 for all spent fuel cases. The subcritical burnup/depletion calculations in ADS are performed until k_{eff} increases to 0.984 in all spent fuel cases and reaching time of this value is determined individually for each case. Subject to this constraint of k_{eff}, the maximum operation times, which mean the end of cycle (EOC), are calculated as 3400, 3270, and 5040 days according to the spent fuel cases of A, B, and C, respectively.

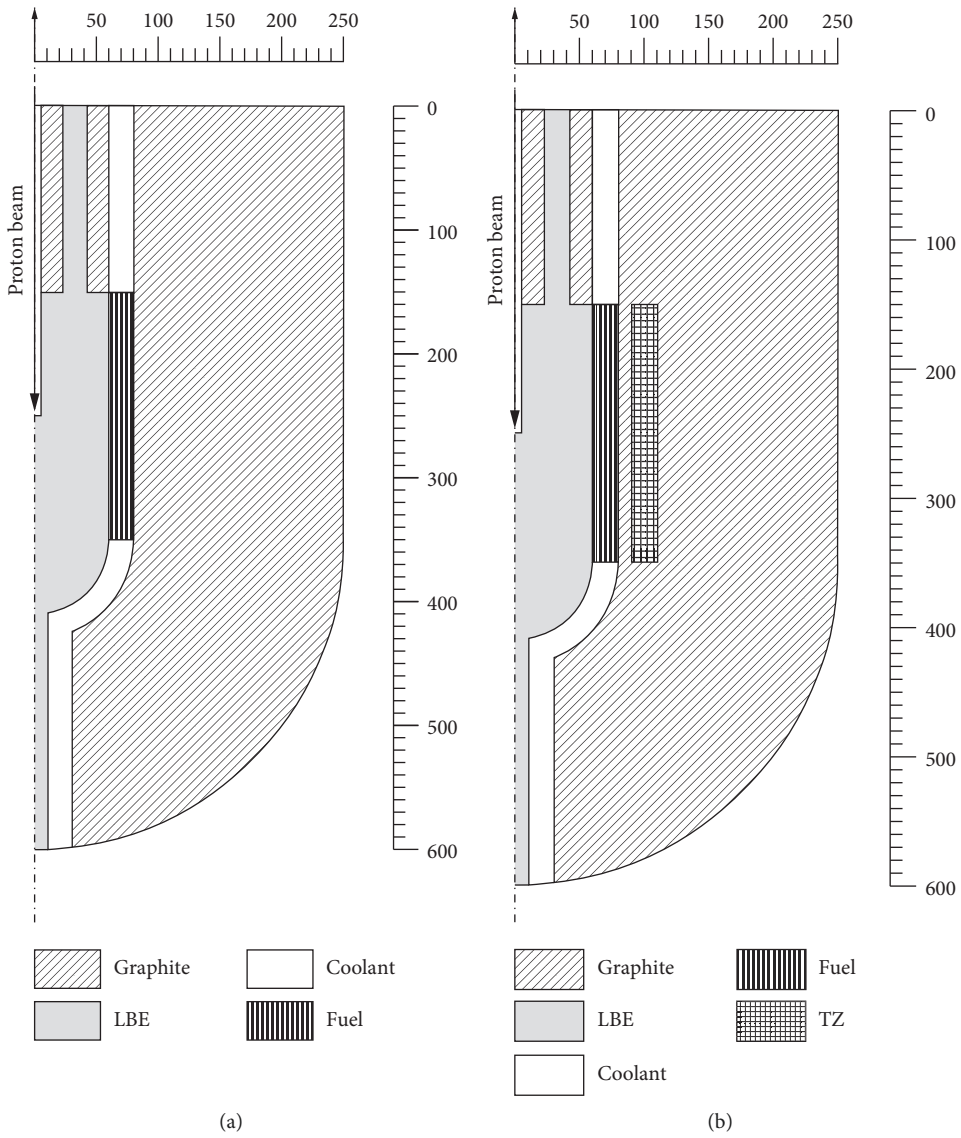

Figure 1: Axisymmetric vertical section views of (a) the original [17] and (b) modified cylindrical ADS (Dimensions are in cm).

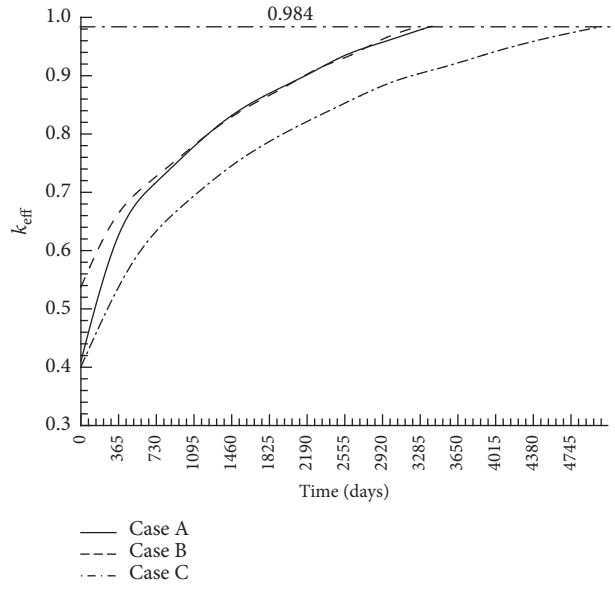

Figure 2: Increase in the effective neutron multiplication factor depending on the operation times.

3.2.2. Cumulative Fissile Fuel Enrichment. Cumulative fissile fuel enrichment (CFFE), expressing the quality of nuclear fuel, can be defined as the ratio of the sum of all fissile fuel isotopes to the sum of all fuel isotopes. Figure 3 shows the increase in CFFE for all spent fuel cases during the operation times. CFFE increases during the operation times, and at the end of cycles, its grades reach to 8.35%, 10.83, and 9.6% for the spent fuel cases of A, B, and C, respectively. These values bring out that the nuclear fuels have quite high quality in terms of fuel enrichment and that they can be reused in nuclear reactors that use enriched fuel at high ratios. The value of k_{eff} rises due to the increase of CFFE.

3.2.3. Energy Gain. The energy gain (G) is one of the most important parameters in ADSs and it is proportional to total fission reactions occurring in the subcritical core of ADS. So, G can be defined as the ratio of the total fission energy to proton energy (E_{p}) and is calculated as follows:

$$G = \frac{R_{\text{f}} E_{\text{f}}}{E_{\text{p}}}, \tag{1}$$

where R_{f} is the number of total fission reactions and E_{f} is the energy per fission (200 MeV).

Figure 4 depicts the increase in G for all spent fuel cases during the operation times. Although the values of G are lower than 1 in the first few months, later these values rapidly increase up to 11.99, 8.11, and 7.98 in the spent fuel cases of A, B, and C, respectively. The results show that the values of G are quite high in terms of energy production. This means that the considered ADS generates a significant amount of energy, as well as the transmutation of LLFPs. In this study, in terms of energy, only energy gain is analyzed. The electrical efficiency of ADS can be calculated by means of ref. [23].

3.2.4. Fuel Burnup. Fuel burnup (BU), which is another important parameter in ADSs, is defined as the total generated energy per unit metric fuel mass initially loaded. Unit of BU is generally expressed as GWd/MTU. Its increase depending on operation time (t) can be calculated as follows:

$$\text{BU}(t + \Delta t) = \text{BU}(t) + \frac{\text{fission power}}{\text{MTU}} \Delta t. \tag{2}$$

This equation shows that BU is also directly proportional to the operation time. Figure 5 exhibits the increases in BU for all spent fuel cases during the operation times. The values of BU increase up to 54.792, 41.614, and 65.579GWd/MTU in the spent fuel cases of A, B, and C at the end of operation times, respectively. CANDU and PWR fuel rods have high burnup capability (up to 500 GWd/MTU) (see refs. [16, 24, 25]).

3.2.5. Safeguard Aspects of ^{239}Pu. The variations of ^{239}Pu are plotted depending on the operation times in Figure 6 for all spent fuel cases. As can be seen from this figure, the maximum^{239}Pu percentage is about 93%, and this means that ^{239}Pu percentages are at the acceptable levels of international safeguarding in all spent fuel cases. ^{238}U fraction

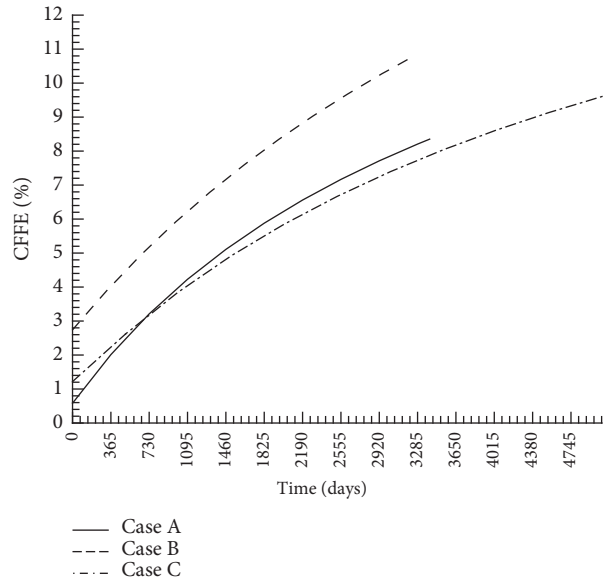

Figure 3: Increase in cumulative fissile fuel enrichment during the operation times.

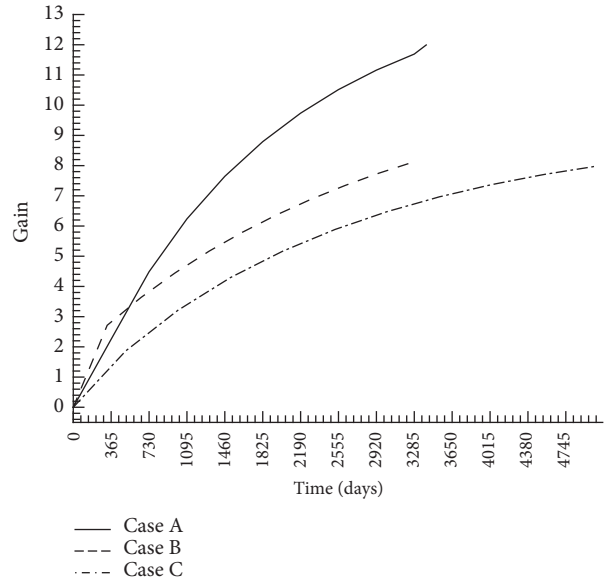

Figure 4: Increase in gain during the operation times.

in CANDU spent fuel (case of A) is higher than in PWR spent fuels (cases of B and C). Therefore, in the case of A, Pu-239 percentage increases first (to around 500 days) and then decreases due to spent Pu-239.

3.3. Transmutation of Fission Products. The transmutation fraction (TF) of a nuclide is the ratio of net transmuted atomic density during the operation time to its atomic density (N) at the beginning of cycle (BOC) and can be calculated as follows:

$$\text{TF} = \frac{N(0) - N(t)}{N(0)}. \tag{3}$$

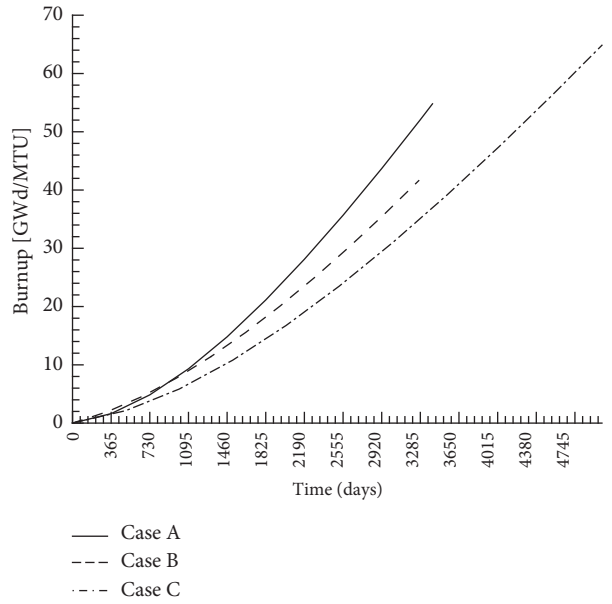

Figure 5: Increase in burnup during the operation times.

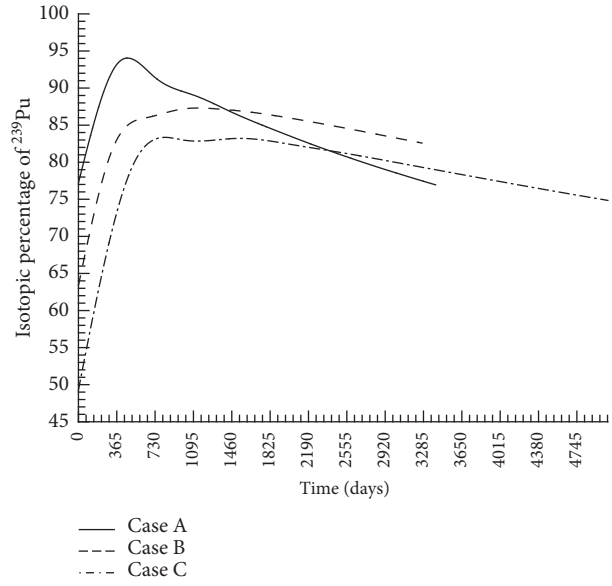

Figure 6: Variation of percentage of ^{239}Pu isotope in plutonium during the operation times.

Atomic densities (N) of isotopes used in the modified ADS are given in Table 1 at the BOC and at the EOC for all spent fuel cases. Furthermore, atomic densities of fission products are given in Tables 2–4 at BOC and EOC for the spent fuel cases of A, B and C, respectively. TFs are also shown in the tables. As is apparent from the tables, among LLFPs, the best transmutation occurs in ^{147}Sm isotope followed by ^{99}Tc and ^{129}I. Its TFs in cases B and C are 54.83% and 81.19%, respectively. Among MLFPs, the best transmutation occurs in ^{147}Pm isotope followed by ^{125}Sb and ^{151}Sm. TFs of ^{147}Pm in cases A, B, and C are 99.82%, 99.38%, and 99.99%, respectively. As expected, MLFPs are more rapidly transmuted with respect to LLFPs because their half-lives are quite shorter than those of LLFPs.

In addition to Tables 2–4, the transmutations of LLFPs and MLFPs during the operation times as mass are plotted in Figures 7 and 8 for all spent fuel cases, respectively. As is apparent from these figures, in the spent fuel cases of A and C, the transmutation profiles decline near to each other. The masses of LLFPs, except ^{147}Sm, decrease gradually and linearly. Although the mass of ^{147}Sm increases slightly in the first few years, later it rapidly decreases. As for the masses of MLFPs, while the masses of ^{125}Sb, ^{147}Pm, and ^{151}Sm decrease exponentially, the masses of ^{90}Sr and ^{137}Cs decrease gradually and linearly.

The numerical results bring out that at the EOC, in the spent fuel case of A, per tHM fuel initially loaded, a total of 0.089 and 0.130 kg of the LLFP and MLFP masses are

Table 1: Atomic densities of isotopes used in the modified ADS (atoms/(barn·cm)).

Isotopes	Case A		Case B		Case C	
	BOC	EOC	BOC	EOC	BOC	EOC
He[a]			8.46569$E-03$			
Cr[b]			3.66345$E-06$			
Fe			7.69324$E-06$			
Zr			3.59861$E-03$			
Sn			5.31202$E-05$			
Hf			3.66345$E-06$			
^{16}O[c]	2.93697$E-02$	1.02789$E-02$	2.73042$E-02$	9.55563$E-03$	2.73680$E-02$	9.57800$E-03$
^{232}Th	—	1.00083$E-09$	9.33110$E-12$	9.33187$E-10$	6.19031$E-03$	1.85725$E-03$
^{233}Pa	—	1.99410$E-11$	—	2.24895$E-11$	—	2.18856$E-06$
^{232}U	—	1.48743$E-09$	—	1.15799$E-09$	—	7.29463$E-08$
^{233}U	—	1.49174$E-09$	—	1.73848$E-09$	2.66993$E-05$	1.71951$E-04$
^{234}U	6.33080$E-07$	1.73443$E-07$	6.11203$E-08$	1.27383$E-07$	6.87464$E-07$	1.43121$E-05$
^{235}U	5.56078$E-05$	7.42546$E-06$	2.46375$E-04$	4.42845$E-05$	8.70822$E-05$	1.29798$E-05$
^{236}U	7.40277$E-06$	4.58373$E-06$	7.30603$E-05$	3.06038$E-05$	4.17128$E-05$	1.52204$E-05$
^{238}U	1.45193$E-02$	4.34139$E-03$	1.26922$E-02$	3.82895$E-03$	6.32613$E-03$	1.81887$E-03$
^{235}Np		3.60106$E-13$	—	9.11276$E-12$	—	1.73780$E-12$
^{236}Np		2.59177$E-11$	2.43482$E-11$	1.97672$E-11$	3.34642$E-12$	3.10285$E-12$
^{237}Np	2.12823$E-07$	8.49462$E-07$	6.13307$E-06$	5.79906$E-06$	3.20538$E-06$	3.44686$E-06$
^{236}Pu		4.56934$E-12$	—	1.82719$E-11$	—	1.46943$E-11$
^{237}Pu		1.01802$E-11$	—	1.19406$E-11$	—	5.84736$E-12$
^{238}Pu	1.71122$E-08$	1.19518$E-06$	2.00245$E-06$	3.22821$E-06$	1.23440$E-06$	2.74465$E-06$
^{239}Pu	2.82080$E-05$	3.52240$E-04$	9.21538$E-05$	4.00820$E-04$	3.10560$E-05$	1.86319$E-04$
^{240}Pu	7.09409$E-06$	6.39388$E-05$	3.01341$E-05$	5.42331$E-05$	2.05142$E-05$	3.84026$E-05$
^{241}Pu	1.02146$E-06$	3.23992$E-05$	1.63268$E-05$	2.28933$E-05$	6.20598$E-06$	1.60207$E-05$
^{242}Pu	1.58382$E-07$	7.33230$E-06$	4.50249$E-06$	4.09549$E-06$	3.81657$E-06$	5.08140$E-06$
^{244}Pu	—	9.79453$E-11$	—	7.07767$E-11$	2.26821$E-11$	1.38317$E-10$
^{241}Am	—	3.79692$E-06$	—	3.62364$E-06$	7.47539$E-07$	3.26888$E-06$
^{243}Am	—	1.29639$E-06$	—	9.88034$E-07$	1.92135$E-07$	1.47667$E-06$
^{242}Cm	—	2.77117$E-07$	—	1.78654$E-07$	1.18948$E-09$	1.76447$E-07$
^{244}Cm	—	3.61448$E-07$	—	3.30190$E-07$	1.33784$E-08$	5.93151$E-07$
^{245}Cm	—	1.45861$E-08$		2.61196$E-08$	1.50500$E-10$	4.43606$E-08$
^{246}Cm	—	2.26875$E-09$	—	1.67286$E-09$	4.11277$E-12$	8.08843$E-09$
^{247}Cm	—	3.13581$E-11$	—	3.40359$E-11$	—	2.00524$E-10$
^{248}Cm	—	1.68813$E-12$	—	1.43607$E-12$	—	1.52560$E-11$
^{206}Pb[d]			3.56020$E-3$			
^{207}Pb			3.39702$E-3$			
^{208}Pb			7.87694$E-3$			
^{209}Bi			1.55345$E-2$			
^{12}C[e]			1.05402$E-1$			

[a]Coolant; [b]clad; [c]fuel; [d]target; [e]reflector.

Table 2: Atomic densities of fission products in the spent fuel case of A (atoms/(barn·cm)) and transmutation fractions (%).

Isotopes	BOC	EOC	TF
C[a]	8.46569$E-03$		
Cr[b]	3.66345$E-06$		
Fe	7.69324$E-06$		
Zr	3.59861$E-03$		
Sn	5.31202$E-05$		
Hf	3.66345$E-06$		
^{88}Sr[c] (ST)	1.73765$E-06$	1.73894$E-06$	
^{89}Sr (SL)	4.17626$E-11$	3.22675$E-12$	
^{90}Sr (ML)	2.70978$E-06$	2.13971$E-06$	21.03
^{89}Y (ST)	—	8.81567$E-09$	
^{90}Zr (ST)	1.85165$E-03$	1.85105$E-03$	
^{91}Zr (ST)	4.03607$E-04$	3.97750$E-04$	
^{99}Tc (LL)	3.62103$E-06$	2.25444$E-06$	37.74

Table 2: Continued.

Isotopes	BOC	EOC	TF
^{100}Ru (ST)	—	1.31173$E-06$	
^{104}Pd (ST)	1.30969$E-07$	1.28054$E-07$	
^{105}Pd (ST)	1.17725$E-06$	8.60523$E-07$	
^{106}Pd (ST)	1.00644$E-06$	1.31348$E-06$	
^{107}Pd (LL)	6.86575$E-07$	6.19016$E-07$	9.839
^{108}Pd (ST)	4.17626$E-07$	3.48791$E-07$	
^{110}Pd (ST)	1.28682$E-07$	1.27669$E-07$	
^{107}Ag (ST)	—	4.97820$E-13$	
^{109}Ag (ST)	—	4.99890$E-08$	
^{111}Cd (ST)	—	6.45046$E-09$	
^{129}I (LL)	4.76286$E-07$	3.24609$E-07$	31.84
^{130}Xe (ST)	—	1.45070$E-07$	
^{135}Cs (LL)	4.11724$E-07$	3.46147$E-07$	15.92
^{137}Cs (ML)	3.72617$E-06$	3.00306$E-06$	19.40
^{136}Ba (ST)	—	6.50100$E-08$	
^{138}Ba (ST)	—	2.88911$E-08$	
^{140}Ce (ST)	3.72986$E-06$	3.70118$E-06$	
^{141}Ce (SL)	—	3.92053$E-10$	
^{142}Ce (LL)	3.42992$E-06$	3.38591$E-06$	1.283
^{143}Ce (SL)	—	2.56216$E-11$	
^{144}Ce (SL)	4.28694$E-07$	1.08340$E-10$	
^{141}Pr (ST)	—	2.61491$E-08$	
^{143}Nd (ST)	—	1.12895$E-08$	
^{147}Pm (ML)	6.42673$E-07$	1.09998$E-09$	99.82

[a]Graphite container; [b]clad; [c]fission products. The abbreviations ST, LL, ML, and SL indicate stable, long-lived, medium-lived, and short-lived fission products, respectively.

Table 3: Atomic densities of fission products in the spent fuel case of B (atoms/(barn·cm)) and transmutation fractions (%).

Isotopes	BOC	EOC	TF
C[a]		8.46569$E-03$	
Cr[b]		3.66345$E-06$	
Fe		7.69324$E-06$	
Zr		3.59861$E-03$	
Sn		5.31202$E-05$	
Hf		3.66345$E-06$	
^{88}Sr[c] (ST)	1.36800$E-05$	1.36796$E-05$	
^{89}Sr (SL)	6.47571$E-11$	1.25672$E-11$	
^{90}Sr (ML)	2.04294$E-05$	1.63956$E-05$	19.74
^{89}Y (ST)	—	1.12758$E-08$	
^{90}Zr (ST)	1.85136$E-03$	1.85419$E-03$	
^{91}Zr (ST)	4.03853$E-04$	4.00924$E-04$	
^{99}Tc (LL)	2.65500$E-05$	1.89445$E-05$	28.64
^{100}Ru (ST)	—	7.46619$E-06$	
^{104}Pd (ST)	4.98160$E-06$	4.84518$E-06$	
^{105}Pd (ST)	9.97799$E-06$	8.35327$E-06$	
^{106}Pd (ST)	7.72943$E-06$	9.38059$E-06$	
^{107}Pd (LL)	5.22938$E-06$	4.61549$E-06$	11.73
^{108}Pd (ST)	3.22306$E-06$	2.84428$E-06$	
^{110}Pd (ST)	1.02480$E-06$	1.01459$E-06$	
^{107}Ag (ST)	—	4.15609$E-12$	
^{109}Ag (ST)	—	4.81870$E-07$	
^{111}Cd (ST)	—	3.25854$E-08$	
^{121}Sb (ST)	8.60222$E-08$	1.77284$E-07$	
^{123}Sb (ST)	1.15609$E-07$	1.01830$E-07$	
^{125}Sb (ML)	1.19751$E-07$	1.22670$E-08$	89.75
^{122}Te (ST)	—	2.93316$E-08$	
^{124}Te (ST)	—	1.43292$E-08$	
^{126}Te (ST)	—	4.04414$E-09$	

Table 3: Continued.

Isotopes	BOC	EOC	TF
^{127}I (ST)	1.11651$E-06$	8.85433$E-07$	
^{129}I (LL)	3.69607$E-06$	3.13893$E-06$	15.07
^{128}Xe (ST)	—	2.04772$E-07$	
^{130}Xe (ST)	—	5.49405$E-07$	
^{140}Ce (ST)	—	1.98972$E-14$	
^{143}Nd (ST)	—	1.60431$E-12$	
^{147}Pm (ML)	2.36469$E-06$	1.44262$E-08$	99.38
^{147}Sm (LL)	2.96344$E-06$	1.33832$E-06$	54.83
^{148}Sm (ST)	2.09656$E-06$	5.33606$E-06$	
^{149}Sm (ST)	8.66879$E-08$	9.75907$E-10$	
^{150}Sm (ST)	5.91357$E-06$	3.22586$E-06$	
^{151}Sm (ML)	3.09584$E-07$	4.60197$E-08$	85.13
^{152}Sm (ST)	2.15869$E-06$	7.12496$E-07$	
^{154}Sm (ST)	6.94169$E-07$	6.48227$E-07$	
^{153}Eu (ST)	—	1.37988$E-06$	
^{155}Gd (ST)	—	1.29399$E-09$	

[a]Graphite container; [b]clad; [c]fission products. The abbreviations ST, LL, ML, and SL indicate stable, long-lived, medium-lived, and short-lived fission products, respectively.

Table 4: Atomic densities of fission products in the spent fuel case of C (atoms/(barn·cm)) and transmutation fractions (%).

Isotopes	BOC	EOC	TF
C[a]		8.46569$E-03$	
Cr[b]		3.66345$E-06$	
Fe		7.69324$E-06$	
Zr		3.59861$E-03$	
Sn		5.31202$E-05$	
Hf		3.66345$E-06$	
^{88}Sr[c](ST)	1.60739$E-06$	1.60972$E-06$	
^{90}Sr (ML)	2.43211$E-06$	1.71430$E-06$	29.51
^{89}Y (ST)	—	1.51207$E-08$	
^{91}Zr (ST)	4.03875$E-04$	3.95236$E-04$	
^{99}Tc (LL)	3.59763$E-06$	1.78287$E-06$	50.44
^{100}Ru (ST)	—	1.70554$E-06$	
^{105}Pd (ST)	1.60923$E-06$	1.00368$E-06$	
^{106}Pd (ST)	1.29609$E-06$	1.87346$E-06$	
^{107}Pd (LL)	1.03754$E-06$	8.79141$E-07$	15.26
^{108}Pd (ST)	6.88986$E-07$	5.18065$E-07$	
^{107}Ag (ST)	—	9.60529$E-13$	
^{109}Ag (ST)	—	8.18027$E-08$	
^{129}I (LL)	5.46246$E-07$	3.11467$E-07$	42.98
^{130}Xe (ST)	—	2.19691$E-07$	
^{140}Ce (ST)	—	4.22066$E-15$	
^{143}Nd (ST)	—	7.44922$E-15$	
^{147}Pm (ML)	6.62429$E-07$	5.26757$E-11$	99.99
^{147}Sm (LL)	5.13789$E-07$	9.66212$E-08$	81.19
^{150}Sm (ST)	6.94149$E-07$	1.27528$E-07$	
^{152}Sm (ST)	4.99773$E-07$	4.17034$E-08$	
^{153}Eu (ST)	—	6.50729$E-08$	

[a]Graphite container; [b]clad; [c]fission products. The abbreviations ST, LL, ML, and SL indicate stable, long-lived, medium-lived, and short-lived fission products, respectively.

transmuted, respectively. These transmutation values are 0.669 and 0.451 kg in the spent fuel case of B, and are 0.179 and 0.100 kg in the spent fuel case of C.

Tritium (^{3}H) is not analyzed due to the fact that the calculations bring out that production of (H-3) is very smaller than other FPs (3.22089$E-01$ gram at the end of EOC in the PWR spent fuel case).

Furthermore, FPs occurring in the subcritical fuel zone during the operation times are analyzed as well as the transmutation of FPs extracted from the thermal reactors.

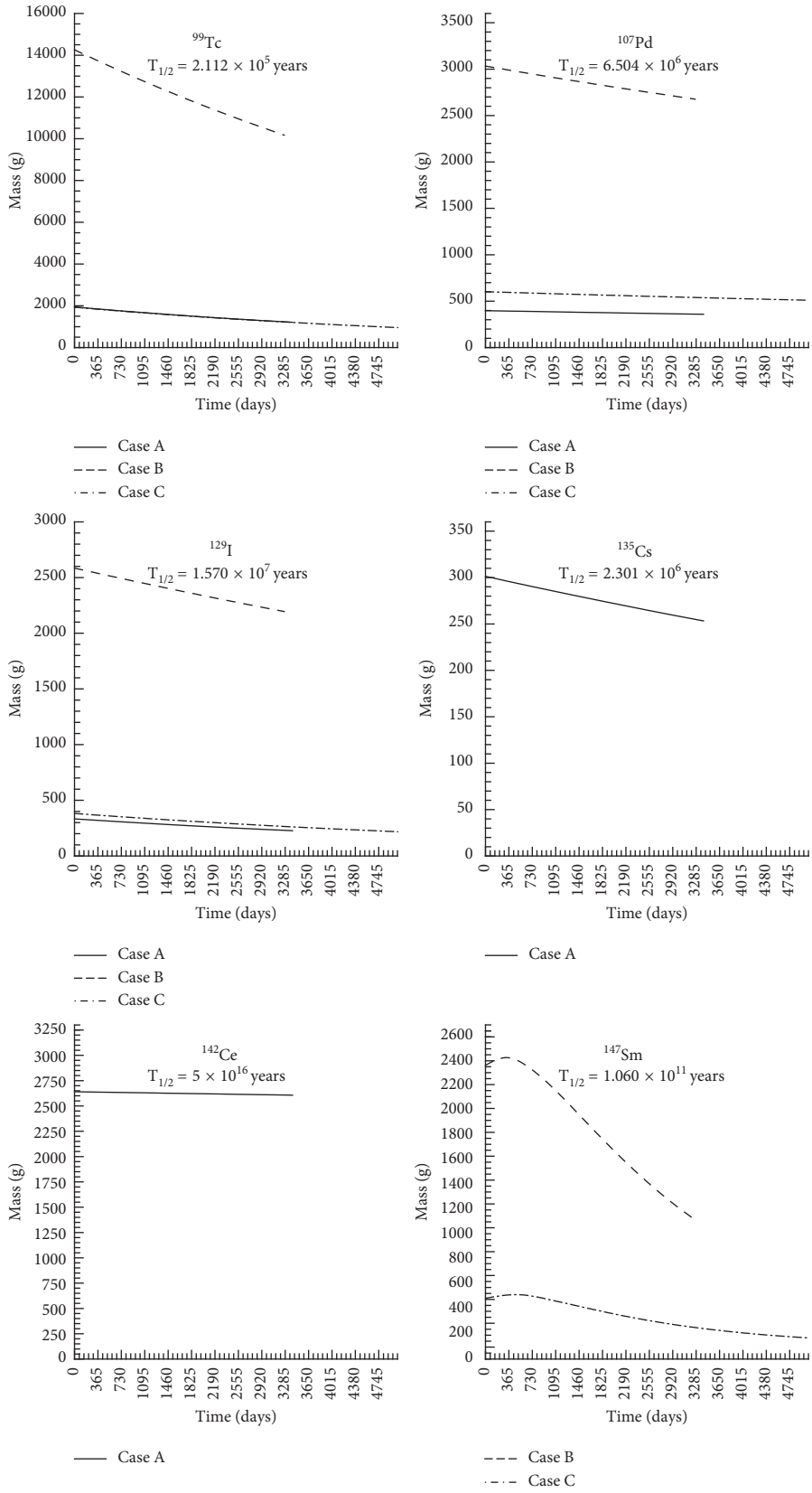

Figure 7: Decrease of masses of LLFPs during the operation times.

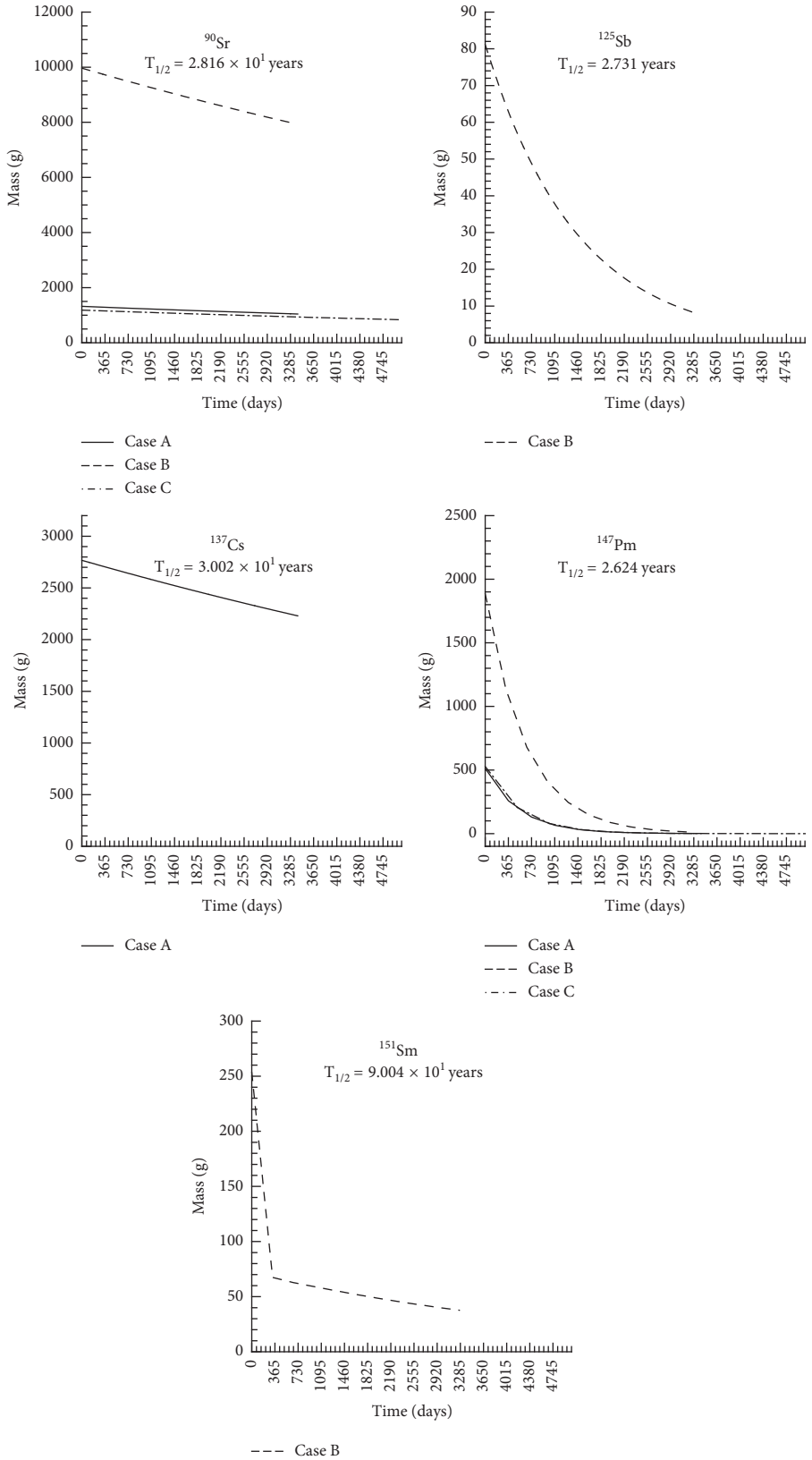

Figure 8: Decrease in masses of MLFPs during the operation times.

Table 5: Production of FPs in the subcritical fuel zone at the end of operation times (gr).

Isotopes	Case A	Case B	Case C
^{90}Sr	1.61038	1.09075	1.18755
^{99}Tc	2.17048	2.02432	2.23503
^{107}Pd	2.59880	2.08753	2.71880
^{125}Sb	—	0.64139	—
^{129}I	2.44305	1.52877	1.95597
^{135}Cs	1.71003	—	—
^{137}Cs	1.81245	—	—
^{142}Ce	1.48112	—	—
^{147}Pm	0.28013	0.33734	0.19971
^{147}Sm	—	0.43720	0.36509
^{151}Sm	—	0.22679	—
Total	14.1064	8.37410	8.66215

Production of FPs in the subcritical fuel zone at the end of operation times is given in Table 5 for all spent fuel cases. As is apparent from this table and Figures 7 and 8, masses of FPs occurring in the subcritical fuel zone are quite less than the amount of transmuted FPs in TZ. This means that FPs can be effectively transmuted in all spent fuel cases.

4. Conclusions

The numerical results obtained from the neutronic analyses of the ADS modified for the transmutations of LLFPs and MLFPs extracted from the CANDU and PWR spent fuels are outlined below briefly:

The modified ADS can be operated safely in the subcritical mode ($k_{\text{eff}} \leq 0.984$) for 3400, 3270, and 5040 days according to the spent fuel cases of A, B, and C, respectively

The grades of CFFEs reach quite high at the end of operation times. This means that the nuclear fuels obtained from the modified ADS can be reused in nuclear reactors that use enriched fuel at high ratios

The values of G are in the range of 7.98 and 11.99, and these values are quite high in terms of energy production

^{239}Pu percentages (<93%) are at the acceptable levels of international safeguarding in all spent fuel cases

The transmutation in most of the considered FPs (especially ^{99}Tc, ^{129}I, ^{147}Sm, ^{147}Pm, ^{125}Sb, and ^{151}Sm) can be effectively realized

Consequently, the considered ADS generates a significant amount of energy along with the transmutations of LLFPs and MLFPs.

Data Availability

The data used to support the findings of this study are available from the corresponding author upon request.

Conflicts of Interest

The authors declare that they have no conflicts of interest.

Acknowledgments

This study was supported by the Research Fund of the Erciyes University (Project no. FDK-2017-7579).

References

[1] H. Yapıcı and G. Özışık, "Modification of PROMETHEUS reactor as a fusion breeder and fission product transmuter," *Journal of Fusion Energy*, vol. 27, no. 4, pp. 256–270, 2008.

[2] H. Yapıcı, N. Demir, and G. Genç, "Neutronic analysis for transmutation of minor actinides and long-lived fission products in a fusion-driven transmuter (FDT)," *Journal of Fusion Energy*, vol. 25, no. 3-4, pp. 225–239, 2006.

[3] H. Yapıcı, N. Demir, and G. Genç, "Time-dependent neutronic analysis for high level waste transmutation in a fusion-driven transmuter," *Journal of Fusion Energy*, vol. 27, no. 3, pp. 206–215, 2007.

[4] M. Igashira and T. Ohsaki, "Neutron economy and nuclear data for transmutation of long-lived fission products," *Progress in Nuclear Energy*, vol. 40, no. 3-4, pp. 555–560, 2002.

[5] K. Liu, H. Wu, L. Cao, and Y. Zheng, "Studies on LLFP transmutation in a pressurized water reactor," *Journal of Nuclear Science and Technology*, vol. 50, no. 6, pp. 581–598, 2013.

[6] M. B. Setiawan and A. Kitamoto, "Study on multi-recycle transmutation of LLFP in light water reactor," *Annals of Nuclear Energy*, vol. 28, no. 18, pp. 1789–1797, 2001.

[7] T. Wakabayashi, "Transmutation characteristics of MA and LLFP in a fast reactor," *Progress in Nuclear Energy*, vol. 40, no. 3-4, pp. 457–463, 2002.

[8] K. Kora, H. Nakaya, H. Matsuura, M. Goto, S. Nakagawa, and S. Shimakawa, "A study on transmutation of LLFPs using various types of HTGRs," *Nuclear Engineering and Design*, vol. 300, pp. 330–338, 2016.

[9] A. Takibayev, M. Saito, V. Artisyuk, and H. Sagara, "Fusion-driven transmutation of selected long-lived fission products," *Progress in Nuclear Energy*, vol. 47, no. 1–4, pp. 354–360, 2005.

[10] B. Sarer, M. E. Korkmaz, M. Günay, and A. Aydın, "Monte Carlo studies in accelerator-driven systems for transmutation of high-level nuclear waste," *Energy Conversion and Management*, vol. 49, no. 7, pp. 1966–1971, 2008.

[11] S. Kawase, K. Nakano, and Y. Watanabe, "Study of proton- and deuteron-induced spallation reactions on the long-lived fission product ^{93}Zr at105 MeV/nucleon in inverse kinematics," *Progress of Theoretical and Experimental Physics*, vol. 2017, no. 9, pp. 1–10, 2017.

[12] C. Y. Han, M. Saito, and H. Sagara, "Transmutation of ^{126}Sn in spallation targets of accelerator-driven systems," *Journal of Nuclear Science and Technology*, vol. 46, no. 1, pp. 60–75, 2009.

[13] W. S. Yang, Y. Kim, R. N. Hill, T. A. Taiwo, and H. S. Khalil, "Long-lived fission product transmutation studies," *Nuclear Science and Engineering*, vol. 146, no. 3, pp. 291–318, 2004.

[14] P. A. Landeyro and M. Guidotti, "Accelerator-driven systems; their application to the incineration of long-lived radioactive waste," *Journal of Nuclear Science and Technology*, vol. 34, no. 2, pp. 156–166, 1997.

[15] H. Yapici, G. Genç, and N. Demir, "A comprehensive study on neutronics of a lead-bismuth eutectic cooled accelerator-driven sub-critical system for long-lived fission product transmutation," *Annals of Nuclear Energy*, vol. 35, no. 7, pp. 1264–1273, 2008.

[16] A. B. Arslan, G. Bakır, G. Genç, and H. Yapıcı, "Analyses of short and long-lived fission products occurring in CANDU

and PWR reactors for medical therapy and diagnosis," in *Proceedings of the 4th International Conference on Computational and Experimental Science and Engineering (ICCESEN-2017)*, p. 12, Antalya, Turkey, October 2017.

[17] G. Bakır and H. Yapıcı, "Time-dependent neutronic and burn-up analyses of in a thorium-based ADS cooled with various coolants," in *Proceedings of the 1st International Symposium on Multidisciplinary Studies and Innovative Technologies Proceedings Book*, pp. 60–64, Tokat, Turkey, November 2017.

[18] D. B. Pelowitz, *MCNPX User's Manual, Version 2.7.0, LA-CP-11-00438*, Los Alamos Scientific Laboratory, Los Alamos, NM, USA, 2011.

[19] M. B. Chadwick, P. G. Young, S. Chiba et al., "Cross-section evaluations to 150 MeV for accelerator-driven systems and implementation in MCNPX," *Nuclear Science and Engineering*, vol. 131, no. 3, pp. 293–328, 1999.

[20] W. B. Wilson, *Manual for CINDER'90 Version 07.4 Codes and Data, LA-UR-07-8412*, Los Alamos Scientific Laboratory, Los Alamos, NM, USA, 2007.

[21] H. Yapici, *XBURN Interface Computer Code for Evaluation of Time-dependent MCNPX 2.7 Outputs*, Erciyes University, Kayseri, Turkey, 2017.

[22] H. Yapıcı, *CBURN Interface Computer Code for Evaluation of Time-dependent CINDER90 Outputs*, Erciyes University, Kayseri, Turkey, 2017.

[23] M. J. Tahar, F. Méot, and S. Peggs, "TUPOY044 energy efficiency of high power accelerators for ADS applications," in *Proceedings of the IPAC2016*, Busan, South Korea, May 2016.

[24] IAEA, "Status and prospects of thermal breeders and their effect on fuel utilization," Technical Report Series No. 195, International Atomic Energy Agency, Vienna, Austria, 1979.

[25] K. S. Allen, "Advanced polymeric burnable poison rod assemblies for pressurized water reactors," Partial Fulfillment of the Requirements for the Degree of Master of Science, A Thesis Presented to the Graduate School of the University of Florida, University of Florida, Gainesville, FL, USA, 2003.

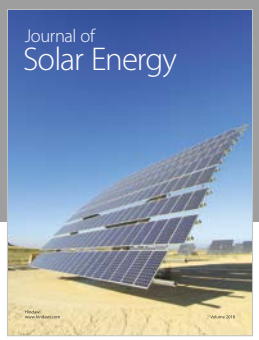



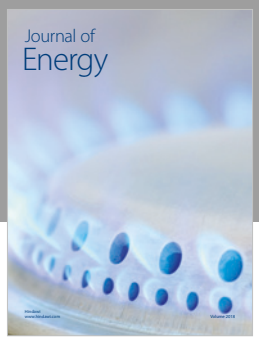

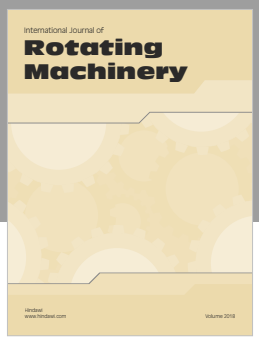

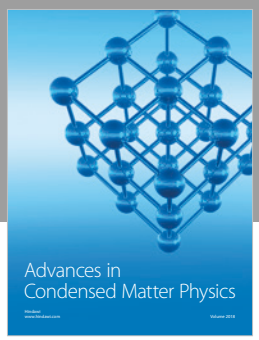



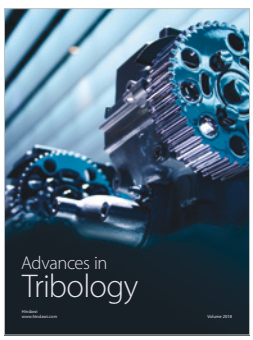

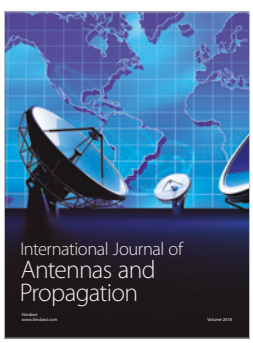

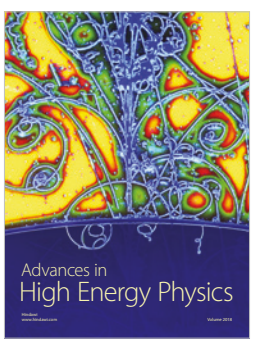

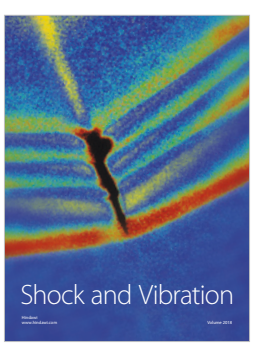



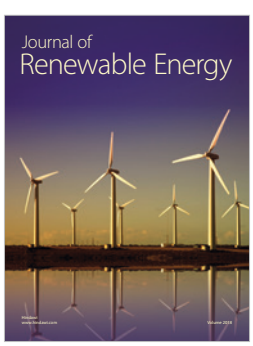

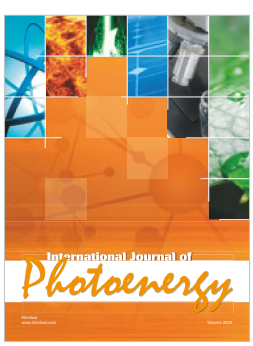



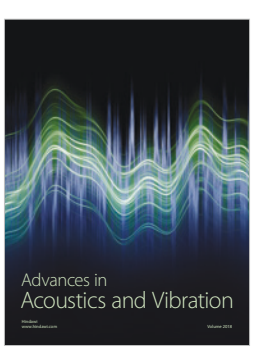

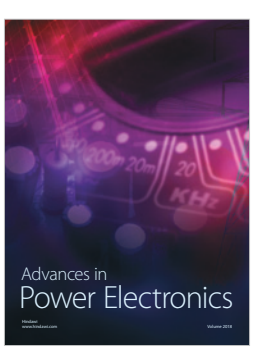



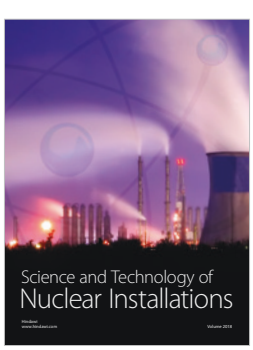



Hindawi

Submit your manuscripts at
www.hindawi.com